Technical Physics, 2024, Vol. 69, No. 2

07

Delay line modelling on exchange spin waves

© V.V. Tikhonov, V.A. Gubanov, A.S. Ptashenko, A.V. Sadovnikov

Saratov National Research State University,
410012 Saratov, Russia
e-mail: tvlad4@yandex.ru

Received August 8, 2023
Revised November 27, 2023
Accepted November 28, 2023

A new innovative device has been proposed — a miniature controlled microwave signal delay line based on short-wave exchange spin waves (ESW). The delay line is based on a three-layer dielectric–ferrite–dielectric epitaxial structure. The conversion of the electromagnetic signal into ESW is carried out in a thin transition layer at the dielectric–ferrite boundary. ESW propagates in the transverse direction of the ferrite layer and is again converted into an electromagnetic signal in the transition layer at the opposite ferrite–dielectric boundary. The duration of the delay of the passed signal is determined by the thickness of the ferrite layer and can be controlled by an external magnetic field. It has been shown that in a three-layer structure based on epitaxial films of gadolinium gallium garnet grown on a substrate of yttrium iron garnet (YIG), the delay duration of the microwave signal can reach several tens of nanoseconds with a YIG layer thickness of 100 mm.

Keywords: spin waves, yttrium iron garnet, gadolinium gallium garnet, microwave signal delay.

DOI: 10.21883/0000000000

Introduction

In modern micro- and nanoelectronics, quantum phenomena in solids are widely used, which served as the basis for research in the field of micromagnetism and nanomagnetism. Of particular interest were studies of spin-wave excitations in magnetically ordered ferrite media. Applied research using short-wave dipole spin waves (in the literature they are more often called „magnetostatic waves“ (MCB)). Based on the MSW, design options for controlled microwave signal delay lines were VHF proposed [1–4]. Including dispersive [1,2] and non-dispersive delay lines [3,4], which were distinguished by their small dimensions and planar structure. In addition, many other microwave devices have been proposed (frequency filters, phase shifters, convolvers and much more). Based on these studies, new scientific directions were formed — spin-wave electronics [5], spintronics [6] and magnonics [7,8]. Further development of these areas was associated with the practical development of ultrashort exchanged spin waves (ESW) with wavelengths of about 100 nm and less 100 nm.

Exchange spin waves were predicted by Bloch back in 1930 [9]. However, until recently, their use was problematic due to the difficulty its generating. The first confirmation of the existence of ESW was obtained only in 1957 [10]. Waves were observed in the form of parametric decay products. Shortly thereafter, spin-wave resonances (SWR) were identified, which were initially observed in thin permalloy films [11,12], and then in epitaxial films of yttrium iron garnet (YIG) [13,14]. The excitation of SWR did not require high localization of magnetic fields. They could be excited even in a uniform UHF magnetic field, but this required „spins pinning on the surface film [15].

In papers [16,17] another mechanism of ESW excitation was proposed, based on the transformation of electromagnetic and exchange spin waves in heterogeneous magnetic fields. The field nonuniformity could be induced by demagnetization fields in bulk ferrite samples or by the nonuniformity of magnetic properties of ferrite films. In the works [18,19], the excitation of traveling OSWs was discovered, which was observed in YIG films pre-implanted with helium ions. The waves were excited in the implanted layer, propagated deep into the YIG film, and reflected from its opposite surface. In the pulse mode, they could be observed as a regular series of delayed ESW echo pulses. In this case, the conversion efficiency of ESW reached 80%, and the temporary attenuation did not exceed the attenuation of magnetostatic waves. Similar results were obtained in specially made YIG films with a smoothly varying magnetization over the entire thickness of the film [20,21].

At the same time, it was known that epitaxial YIG films grown on gadolinium gallium garnet (GGG) substrates have their own magnetic inhomogeneity22-24. At the film-substrate interface, a thin transition layer (TS) is always formed, in which the magnetization of the film smoothly increases from zero to the magnetization of pure YIG. The existence of a transition layer made it possible to detect effective excitation of ESW in serial samples of YIG films without any additional influences [25,26].

The high efficiency of ESW conversion in the transition layer of the YIG film opened up broad opportunities for the creation of fundamentally new spin-wave devices. However, this required spatial separation of the points of excitation and reception of OSW. This requirement was satisfied by using a three-layer film structure GGG–YIG–GGG, as, for example, in the delay line at OSW [27]. The GGG film on the outer surface of the YIG film was only necessary to create the second transition layer; its thickness was not significant. The time delay of the transmitted signal was determined by the propagation speed and the path length of the ESW in the transverse direction of the YIG film. However, in the case of a thin YIG film, this circumstance significantly limited the possibility of achieving a long delay of the microwave signal.

In this work, the possibility of a multiple increase in the delay time was investigated. For this purpose, a modernized three-layer GGG-YIG-GGG structure was studied, consisting of a YIG substrate on the opposite surfaces of which GGG epitaxial films were located.

1. Delay Line Simulation

It was believed that during the epitaxial growth of GGG films, thin transition layers are formed on the surfaces of the YIG substrate, caused by the diffusion of non-magnetic ions Gd^{3+} from the Ga^{3+} GGG film ($Gd_3Ga_5O_{12}$), partially replacing the Y^{3+} and Fe^{3+} in the YIG substrate ($Y_3Fe_5O_{12}$). Since GGG films are needed only for creating transition layers, the simplest epitaxy methods can be used for their formation, for example, the magnetron sputtering method [24].

According to the theory of diffusion in solids, the distribution of the concentration of doping ions in the YIG substrate is described by the Gaussian function $N(z) \propto \exp(-z^2/\sigma^2)$, where σ is the phenomenological distribution parameter, z is the coordinate in the transverse direction of the YIG layer. Taking this into account, the distribution of spontaneous magnetization over the thickness of the YIG layer is described by the function

$$M(z) = M_0\left\{1 - \exp\left(-\frac{z^2}{\sigma^2}\right) - \exp\left[-\frac{(z-d)^2}{\sigma^2}\right]\right\}, \quad (1)$$

where M_0 is the magnetization of the substrate outside the transition layer, d is the thickness of the YIG layer.

Fig. 1 shows the geometry for the problem of simulating of delay line, including the processes of excitation, propagation and reception of ESW.

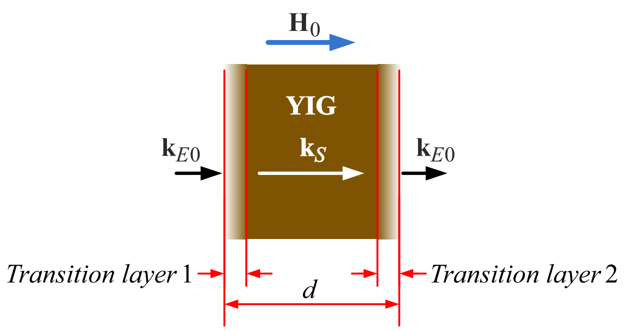

Figure 1. Geometry for the problem of simulating of delay line at ESW.

The case of normal incidence of a plane electromagnetic wave (EMW) on the surface of a normally magnetized YIG layer $\mathbf{H}_0 \parallel \mathbf{k}_0 \parallel \mathbf{z}$ was considered. The dynamics of the magnetization vectors $\mathbf{M}(t,z) = \mathbf{M}(z) + \mathbf{m}(t,z)$, electric field $\mathbf{E}(t,z) = \mathbf{e}(t,z)$ and magnetic field $\mathbf{H}(t,z) = \mathbf{H}_i(z) + \mathbf{h}(t,z)$ were described by the linearized Landau–Lifshitz equation taking into account inhomogeneous exchange

$$\frac{\partial m}{\partial t} + \gamma H_i(z)(\mathbf{m}\times\mathbf{z}) + \gamma M(z)(\mathbf{m}\times\mathbf{h}) + \eta(\mathbf{z}\times\nabla^2\mathbf{m}) = 0 \quad (2)$$

and Maxwell's system of equations

$$\nabla\times\mathbf{e} = -\frac{1}{c}\frac{\partial}{\partial t}(\mathbf{h}+4\pi\mathbf{m}),$$
$$\nabla\times\mathbf{h} = \frac{\varepsilon}{c}\frac{\partial\mathbf{e}}{\partial t},$$
$$\nabla\cdot\mathbf{e} = 0,$$
$$\nabla\cdot(\mathbf{h}+4\pi\mathbf{m}) = 0, \quad (3)$$

where $H_i(z) = H_0 - 4\pi M(z)$ is internal field of the YIG layer, $\gamma = 1.76\cdot 10^7\,\mathrm{Oe}^{-1}\cdot\mathrm{s}^{-1}$ is gyromagnetic ratio, $\eta = 8.62\cdot 10^6\,\mathrm{cm}^2\cdot\mathrm{s}^{-1}$ is inhomogeneous exchange constant, $\varepsilon = 14E$ is relative dielectric constant of YIG.

The solution was sought in the form of plane monochromatic waves $\mathbf{e}, \mathbf{h}, \mathbf{m} \propto \exp[i(\omega t - kz)]$, where $\omega = 2\pi f$ is circular frequency, k -is propagation number. In coordinate form, equations (2), (3) split into two independent systems of equations for waves with right-handed $a_+ = a_x + ia_y$ and left-handed circular polarization I$a_- = a_x - ia_y$

$$[\omega \mp (\omega_H + \eta k^2)]m_\pm = -\gamma M h_\pm, \quad (4)$$

$$e_\pm = i\frac{4\pi k_0 k}{k^2 - \varepsilon k_0^2}m_\pm, \quad h_\pm = \frac{4\pi\varepsilon k_0^2}{k^2-\varepsilon k_0^2}m_\pm, \quad (5)$$

where $k_0 = \omega/c$ is wave number for EMW in vacuum. The longitudinal components of the vectors $\mathbf{e}$, $\mathbf{h}$, $\mathbf{m}$ were turned to zero ($e_z, h_z, m_z = 0$).

Subsequently, we were only interested in right-hand polarized waves that coincided with the direction precession of the magnetization vector. By substituting the expression h_+ from (5) into (4), one obtained the dispersion equation

$$(k^2 - k_{S0}^2)(k^2 - k_{E0}^2) = k_{E0}^2\frac{\omega_M(z)}{\eta}, \quad (6)$$

had a simple analytical solution

$$k_{S,E}(H_0, f, z, \sigma) =$$

$$\pm\sqrt{\frac{1}{2}(k_{S0}^2 + k_{E0}^2) \pm \sqrt{\frac{1}{4}(k_{S0}^2+k_{E0}^2)^2 + k_{E0}^2\frac{\omega_M(z)}{\eta}}}, \quad (7)$$

where$k_{S0}(f,z) = \sqrt{\frac{[\omega-\omega_H(z)]}{\eta}}$ and $k_{E0}(f) = \sqrt{\varepsilon}k_0$ are partial laws of dispersion of ESW and EMW, $\omega_H(z) = \gamma[H_0 - 4\pi M(z)]$, $\omega_M(z) = 4\pi\gamma M(z)$.

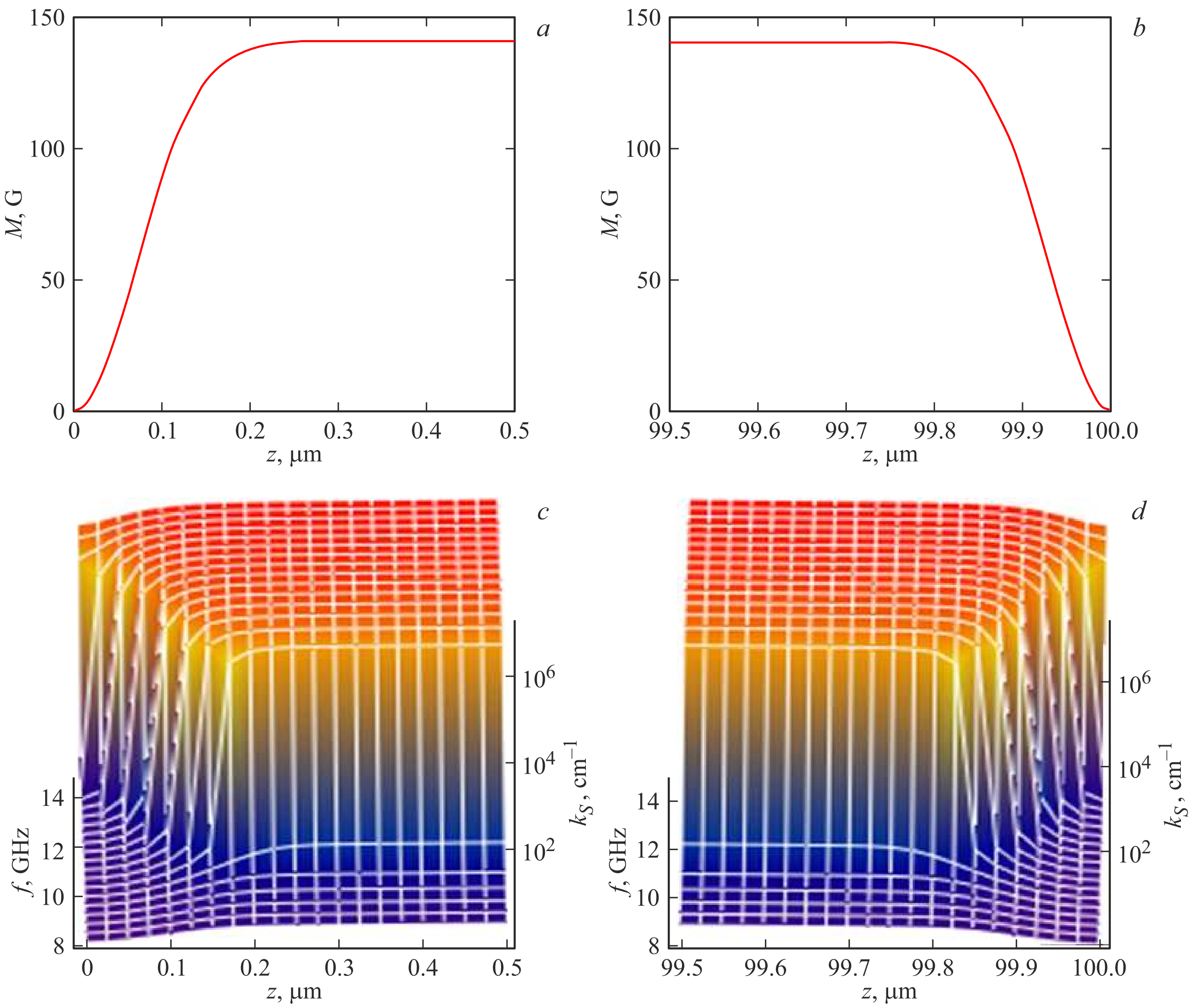

Figure 2. Magnetization distribution in TS1 (a) and TS2 (b), dispersion of hybridized ESW in TS1 (c) and TS2 (d).

Expression (7) described two branches of the dispersion of hybrid electromagnetic spin waves. The sign (+) under the radical corresponded to the dispersion of hybridized ESW$k_S(H_0, f, z, \sigma)$, and the sign (−) corresponded the dispersion of hybridized EMV I$k_E(H_0, f, z, \sigma)$.

The processes of hybridization and transformation of wave types occurred within the thickness of the transition layers, as shown in Fig. 2. Fig. 2, *a, b* shows graphs of the distribution function $M(z)$ in transition layer 1 (TS1) and transition layer 2 (TS2). Similarly, Fig. 2, *c, d* shows 3*d* graphs of hybridized $k_S(f, z)$ ESWs in TS1 and TS2. Calculations were carried out at a given value of $\sigma = 10^{-5}$ and a fixed field $H_0 = 5$ kOe.

It can be seen that in the TS1 layer the EMV was converted into short-wave ESW. In the TS2 layer, the reverse transformation of ESW into EMW occurred. In both cases, the directions of the wave vectors of electromagnetic and exchange spin waves strictly coincided, which meant collinear interaction of coupled waves, providing the most intense energy conversion at hybridization frequencies. In the region of homogeneous magnetization of the YIG layer, the connection between electromagnetic and exchange spin waves ceased, and the waves propagated independently of each other.

It should be noted that a smooth change in magnetization in the transition layers practically eliminates the reflection of waves at the film-substrate boundaries. In this case, the loss of the useful signal due to wave type conversion is reduced to almost zero.

Using expression (7), it was not difficult to calculate the time delay of the transmitted signal over the ESW path length equal to the thickness of the YIG layer

$$\tau(H_0, f) = \frac{1}{2\pi} \int_0^d \frac{\partial}{\partial f} k_S(H_0, f, z) dz, \qquad (8)$$

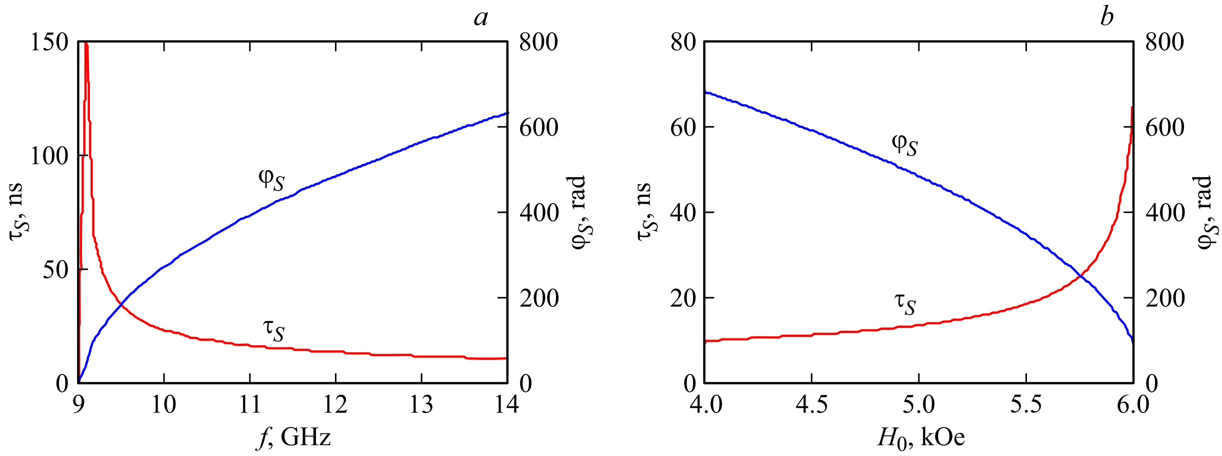

Figure 3. Frequency dependence of the delay time and phase incursion of the ESW at a given field value $H_0 = 5\,\text{kOe}$ (a) and field dependence of the delay time and phase incursion of the ESW at a given frequency value $f = 12\,\text{GHz}$ (b).

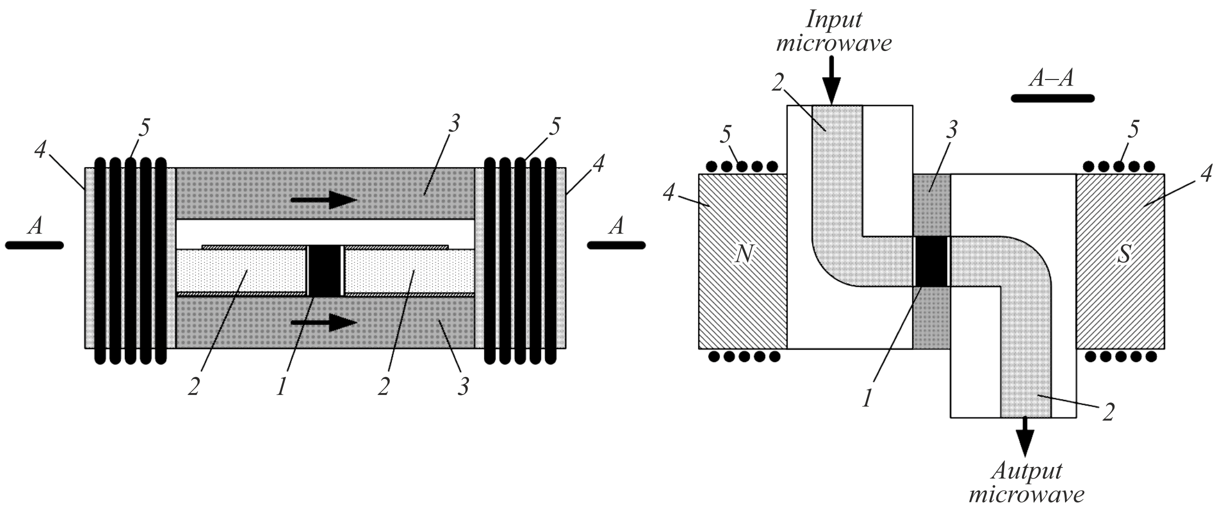

Figure 4. Controlled delay line design at ESW.

as well as the phase shift of the transmitted VHF signal

$$\varphi(H_0, f) = \int_0^d k_S(H_0, f, z)dz. \tag{9}$$

The calculations results are presented in Fig. 3. The graphs in Fig. 3, a show the frequency dependence of the delay time $\tau(f)$ and the phase shift$\varphi(f)$m for a given YIG layer thickness $d = 100\,\mu\text{m}$ and a fixed field value $H_0 = 5\,\text{kOe}$. Fig. 3, b shows the field dependences of $\tau(H_0)$and $\varphi(H_0)$, calculated at a fixed frequency value $f = 12\,\text{GHz}$.

The frequency dependences in Fig. 3, a display the dispersion properties of the delay line, which, obviously, will manifest themselves in the form of distortions of the delayed radio pulse. The field dependences in Fig. 3, b demonstrate the adjustments of the delay time and the phase shift of the transmitted signal.

2. Delay line construction

Fig. 4 shows a variant of the design of a controlled delay line based on exchange spin waves.

The design includes a three-layer GGG–YIG–GGG *1* structure, an input and output microstrip transmission line (MSL) *2* and a portable controlled magnetic system. A sample of the GGG–YIG–GGG structure is installed in the MPL discontinuity so that the flat surfaces of the three-layer structure are closely adjacent to the end surfaces of the input and output MPL (Fig. 5). A sample structure along with the input and output MPL is installed in the working gap of a portable controlled magnetic system.

The magnetic system includes two NdFe35 neodymium magnets with dimensions $8 \times 4 \times 10\,\text{mm}$ *3*, two pole-pieces made of steel Grade St.1008 with dimensions $6 \times 10 \times 10\,\text{mm}$ *4* and two control coils *5*. For given

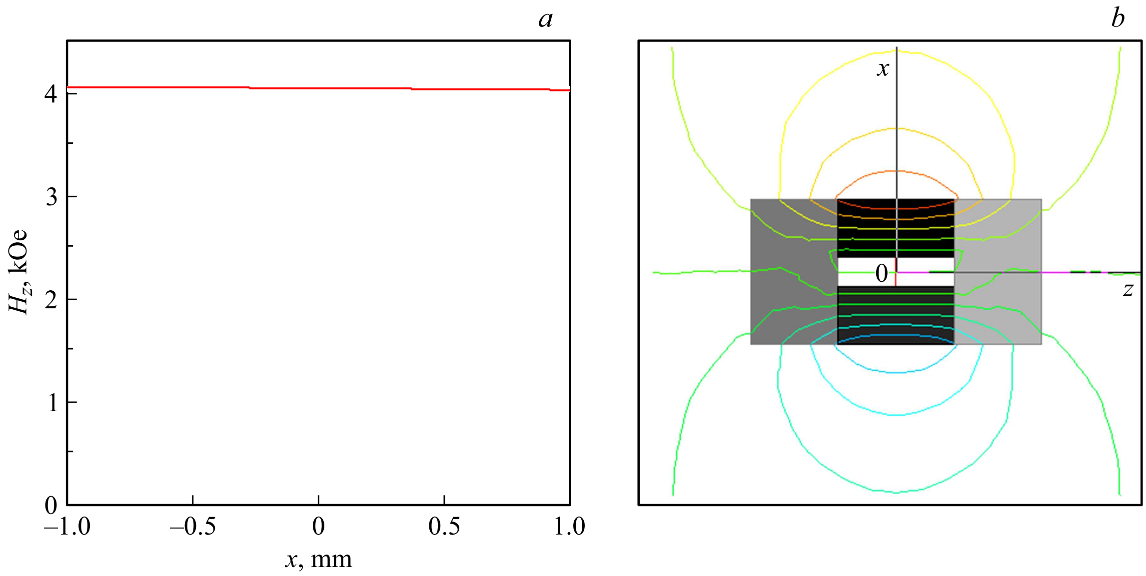

Figure 5. Field topology in the working gap of the magnetization system (a) and the pattern of field lines inside and outside the working gap of the magnetic system (b).

dimensions of the elements of the magnetic system, the topology of the magnetizing fields was calculated.

Calculations were carried out using numerical methods using the Maxwell SV software package. The calculation results are presented in Fig. 5. The graph in Fig. 5, a shows the topology of the magnetizing field in the working gap of the magnetic system. The graph in Fig. 5, b shows calculations of field lines inside and outside the working gap.

It can be seen that with sufficiently small dimensions of the magnetic system, the field strength in the working gap exceeded 4 kOe. In this case, the field was almost uniform, which is especially important for reducing the phase losses of the delayed VHF signal. Additional fields created by control coils do not change the field topology.

Conclusion

Thus, it has been shown that a delay line on an ESW, made on the basis of a modernized GGG–YIG–GGG film structure grown on a single-crystal YIG substrate, multiplies the delay time of the VHF signal. With the thickness of the 100 μm substrate, the delay duration can reach several tens of nanoseconds.

Important advantages of ESW devices are their miniature size, simplicity of design, and manufacturability.

The proposed delay line design can be used in systems for generating and processing radio signals, as well as an electronically variable phase shifter in phased antenna arrays.

Funding

This study was supported financially by the Russian Science Foundation (project № 23-79-30027).

Conflict of interest

The authors declare that they have no conflict of interest.

References

[1] Y.K. Fetisov, G. Srinivasan. Appl. Phys. Lett., **87**, 103502 (2005). https://doi.org/10.1063/1.2037860

[2] A.A. Nikitin, A.E. Komlev, A.A. Nikitin, A.B. Ustinov. Izv. vuzov, Prikladnaya nelineynaya dinamika, **30** (5), 605 (2022) (in Russian). DOI: 10.18500/0869-6632-003006

[3] A.B. Ustinov, V.E. Demidov, B.A. Kalinikos. Electron. Lett., **37** (19), 1161 (2021). DOI: 10.1049/el:20010809

[4] S.L. Vysotsky, G.T. Kazakov, A.V. Kozhevnikov, S.A. Nikitov, A.V. Romanov, Yu.A. Filimonov. Pisma v ZhTF, **32** (15), 45 (2006) (in Russian).

[5] Y. Kajiwara, K. Harii, S. Takahashi, J. Ohe, K. Uchida, M. Mizuguchi, H. Umezawa, H. Kawai, K. Ando, K. Takanashi, S. Maekawa, E. Saitoh. Nature, **464**, 262 (2010). https://doi.org/10.1038/nature08876

[6] A. Hirohata, K. Yamada, Y. Nakatani, L. Prejbeanu, B. Diény, P.H. Pirro, B. Hillebrands. J. Magn. Magn. Mater., **509**, 166711 (2020). https://doi.org/10.1016/j.jmmm.2020.166711

[7] S.A. Nikitov, D.V. Kalyabin, I.V. Lisenkov, A.N. Slavin, Yu.N. Barabanenkov, S.A. Osokin, A.V. Sadovnikov, E.N. Beginin, M.A. Morozova, Yu.P. Sharaevsky, Yu.A. Filimonov, Yu.V. Khivintsev, S.L. Vysotsky, V.K. Sakharov, E.S. Pavlov. Phys.-Usp., **58**, 1002 (2015). https://doi.org/10.3367/UFNe.0185.201510m.1099

[8] A. Barman, G. Gianluca, S. Ladak, A.O. Adeyeye, M. Krawczyk, J. Gräfe, C. Adelmann, S. Cotofana, A. Naeemi, V.I. Vasyuchka, B. Hillebrands, S.A. Nikitov, H. Yu, D. Grundler, A.V. Sadovnikov, A.A. Grachev, S.E. Sheshukova, J.-Y. Duquesne, M. Marangolo, G. Csaba, W. Porod, V.E. Demidov, S. Urazhdin, S.O. Demokritov, E. Albisetti, D. Petti, R. Bertacco, H. Schultheiss, V.V. Kruglyak, V.D. Poimanov, S. Sahoo, J. Sinha, H. Yang, M. Münzenberg, T. Moriyama, S. Mizukami, P. Landeros, R.A. Gallardo, G. Carlotti, J.-V. Kim, R.L. Stamps, R.E. Camley, B. Rana, Y. Otani, W. Yu, T. Yu, G.E.W. Bauer, C. Back, G.S. Uhrig, O.V. Dobrovolskiy, B. Budinska, H. Qin, S. van Dijken, A.V. Chumak, A. Khitun, D.E. Nikonov, I.A. Young, B.W. Zingsem, M. Winklhofer. J. Phys. Condens. Matter., **33** (41), 1 (2021). https://doi.org/10.1088/1361-648X/abec1a

[9] F. Bloch. Z. Physik, **61**, 206 (1930). https://doi.org/10.1007/BF01339661

[10] H. Suhl. J. Phys. Chem. Solids, **1**, 209 (1957). https://doi.org/10.1016/0022-3697(57)90010-0

[11] M.H. Seavey, P.E. Tannenwald. Phys. Rev. Lett., **1**, 168 (1958). https://link.aps.org/doi/10.1103/PhysRevLett.1.168

[12] G.T. Rado, J.R. Weertman. J. Phys. Chem. Solids., **11**, 315 (1959). https://doi.org/10.1016/0022-3697(59)90233-1

[13] R.E. De Wames, T. Wolfram. J. Appl. Phys., **41**, 987 (1970). DOI: 10.1063/1.1659049

[14] J.D. Adam, T.W. O'Keeffe, R.W. Patterson. J. Appl. Phys., **50**, 2446 (1979). DOI: 10.1063/1.326980

[15] C. Kittel. Phys. Rev., **110** (6), 1295 (1958). https://doi.org/10.1103/PhysRev.110.836

[16] E. Schlömann. J. Appl. Phys., **35**, 159 (1964). https://doi.org/10.1063/1.1713058

[17] E. Schlomann, R.I. Joseph, T. Kohane. Proceed. IEEE, 53 (1965). DOI: 10.1109/PROC.1965.4262

[18] Yu.V. Gulyaev, P.E. Zilberman, E.S. Sannikov, V.V. Tikhonov, A.V. Tolkachev. Pis'ma v ZhTF **14**, 884 (1988) (in Russian).

[19] V.V. Tikhonov, A.V. Tolkachev. FTT, **36** (1), 185 (1994) (in Russian).

[20] P.E. Zilberman, A.G. Temiryazev, M.P. Tikhomirova. UFN, **38**, 1173 (1995) (in Russian). http://dx.doi.org/10.1070/PU1995v038n10ABEH001493

[21] A.G. Temiryazev, M.P. Tikhomirova, P.E. Zilberman, A.V. Maryakhin. J. Phys. IV France, **7**, 1 (1997). https://doi.org/10.1051/jp4:19971160

[22] M. Shone. Circuits. Syst. Signal Proces., **4**, 89 (1985). https://doi.org/10.1007/BF01600074

[23] S.I. Yushchuk. Tech. Phys., **44** (12), 1454 (1999). https://doi.org/10.1134/1.1259547

[24] M.-B. Park, N.-H. Cho. J. Magn. Magn. Mater., **231**, 253 (2001). https://doi.org/10.1016/S0304-8853(01)00068-3

[25] V.V. Tikhonov, A.N. Litvinenko. Appl. Phys. Lett., **115** (7), 072410 (2019). https://doi.org/10.1063/1.5098116

[26] V.V. Tikhonov, A.N. Litvinenko J. Magn. Magn. Mater., **515**, 167241 (2020). DOI: 10.1016/j.jmmm.2020.167241

[27] *XII Vserossiyskaya nauchno-tekhnicheskaya konferentsiya „Elektronika i mikroelektronika SVCH"*. Collection of reports (St. Petersburg, May 29 – June 2023 St. Petersburg: SPbGETU „Technical University LETII"), 646 p. V.V. Tikhonov, V.A. Gubanov, A.V. Sadovnikov. Elektronika i mikroelektronika SVCH. 600 p. https://mwelectronics.etu.ru/2023/ru/sbornik-dokladov-1

[28] H. Mehrer. *Diffusion in Solids: Fundamentals, Methods, Materials, Diffusion-Controlled Processes* (Springer, 2007)

Translated by V.Prokhorov